

# Regimes Of Helium Burning

F. X. Timmes and J. C. Niemeyer

*Center on Astrophysical Thermonuclear Flashes  
University of Chicago  
Chicago, IL 60637*

## ABSTRACT

The burning regimes encountered by laminar deflagrations and ZND detonations propagating through helium-rich compositions in the presence of buoyancy-driven turbulence are analyzed. Particular attention is given to models of X-ray bursts which start with a thermonuclear runaway on the surface of a neutron star, and the thin shell helium instability of intermediate-mass stars. In the X-ray burst case, turbulent deflagrations propagating in the lateral or radial directions encounter a transition from the distributed regime to the flamlet regime at a density of  $\sim 10^8 \text{ g cm}^{-3}$ . In the radial direction, the purely laminar deflagration width is larger than the pressure scale height for densities smaller than  $\sim 10^6 \text{ g cm}^{-3}$ . Self-sustained laminar deflagrations travelling in the radial direction cannot exist below this density. Similarly, the planar ZND detonation width becomes larger than the pressure scale height at  $\sim 10^7 \text{ g cm}^{-3}$ , suggesting that a steady-state, self-sustained detonations cannot come into existence in the radial direction. In the thin helium shell case, turbulent deflagrations travelling in the lateral or radial directions encounter the distributed regime at densities below  $\sim 10^7 \text{ g cm}^{-3}$ , and the flamelet regime at larger densities. In the radial direction, the purely laminar deflagration width is larger than the pressure scale height for densities smaller than  $\sim 10^4 \text{ g cm}^{-3}$ , indicating that steady-state laminar deflagrations cannot form below this density. The planar ZND detonation width becomes larger than the pressure scale height at  $\sim 5 \times 10^4 \text{ g cm}^{-3}$ , suggesting that steady-state, self-sustained detonations cannot come into existence in the radial direction.

*Subject headings:* hydrodynamics, stars:general, turbulence

## 1. Introduction

Thermonuclear flames fronts are ubiquitous in stellar models of Type Ia supernova, X-ray bursts, and shell flashes of intermediate stars. Flame fronts propagating through carbon and carbon-oxygen compositions are prevalent in Type Ia supernova models (Timmes & Woosley 1992; Khokhlov 1995; Boisseau et al. 1996; Niemeyer & Kerstein 1997), while flame fronts propagating through helium compositions play a pivotal role in X-ray burst models (Fryxell & Woosley

1982; Taam 1987; Taam, Woosley, & Lamb 1996; Zingale et al. 2000) and shell flash models of intermediate-mass stars (Schwarzschild & Härm 1965; Paczynski 1974; Iben 1977; Clayton & De Marco 1997). In this paper we focus on flame fronts propagating through helium compositions.

In most of the X-ray burst and thin shell flash models, the flame front operates in a layer that is thin compared to the radius of the star. Local temperature perturbations in these thin layers become amplified due to the nonlinear temperature dependence of the nuclear reaction rates. Ignition of the flame front probably takes place at an individual point, or a small set of points, rather than simultaneously throughout the entire layer as spherically symmetric models require. The flame front which subsequently propagates through the thin layer may be a detonation, which travels faster than the local sound speed, or a deflagration, which travels slower than the local sound speed. Which type of flame front initially propagates depends primarily on the prevailing thermodynamic conditions and velocity fields. Roughly speaking, the formation of a detonation is suppressed in the presence of strong temperature fluctuations on scales smaller than  $\sim 10^3$  times the detonation width (Montgomery et al. 1998). The detonation or deflagration propagates both laterally around the star and vertically through the thin layer. The duration of a stellar event, or the observed rise time of the luminosity, may be related in a fundamental way to the speed at which the flame front propagates through the thin layer (e.g., Fryxell & Woosley 1982).

Neutron stars which accrete hydrogen-rich material from a binary companion, or from the interstellar medium, end up with a thin layer of helium-rich fuel on their surface. The helium-rich fuel may be spread evenly over the entire neutron star, or the fuel may be confined to the polar regions if the magnetic field is sufficiently strong. For a relatively slow ( $\dot{M} \sim 10^{-11} M_{\odot} \text{ y}^{-1}$ ) accretion rate that is spherically symmetric, a thick layer of helium ( $\sim 10^4 \text{ cm}$ ) develops before ignition. The density at the base of the accreted layer reaches  $\sim 10^8 \text{ g cm}^{-3}$  and the temperature reaches  $\sim 10^8 \text{ K}$  (Woosley & Taam 1976; Brown & Bildsten 1998). At these thermodynamic conditions a planar detonation propagates in the lateral direction (perpendicular to the direction of the gravitational force) at a speed of  $S_D \sim 10^9 \text{ cm s}^{-1}$ , while a purely laminar deflagration propagates in the lateral direction at a speed of  $S_L \sim 10^6 \text{ cm s}^{-1}$  (Timmes 1999). For larger accretion rates ( $\dot{M} \sim 10^{-9} M_{\odot} \text{ y}^{-1}$ ), a thinner layer of helium ( $\sim 10^3 \text{ cm}$ ) is deposited before ignition. The density at the base of this accreted layer is  $\sim 10^6 \text{ g cm}^{-3}$  and the temperature reaches  $\sim 10^8 \text{ K}$  (Wallace, Woosley, & Weaver 1982; Brown & Bildsten 1998). For these thermodynamic conditions, the lateral speed of a self-sustained detonation is  $S_D \sim 10^9 \text{ cm s}^{-1}$ , while a purely laminar deflagration propagates in the lateral direction at a speed of  $S_L \sim 10^4 \text{ cm s}^{-1}$  (Timmes 1999). The vast difference between these estimates for the planar detonation speeds and the purely laminar deflagration speeds imply very different predictions for the rise time of an X-ray burst (e.g., Fryxell & Woosley 1982).

The thin shell helium flash which occurs during the advanced evolutionary stages of intermediate-mass stars (Schwarzschild & Härm 1965) results from nuclear burning being unable to raise the overlying hydrogen envelope sufficiently to extinguish the reactions. A drastic temperature rise at near constant pressure ensues. Shortly after reaching its peak temperature, however, the material

does expand and cool on a rapid timescale. Note that in contrast to the neutron star example, the layer of fuel in the thin shell helium flash is located inside a star rather than on the surface of a star. We will focus on a single model of a helium shell flash, namely, the  $M \sim 1.0M_{\odot}$  core of a  $7 M_{\odot}$  star studied by Iben (1977). Other models tested give qualitatively similar results. Typical shell radii, densities and temperatures at the onset of this thin shell helium flash model are  $R \sim 7 \times 10^8$  cm,  $\rho \sim 10^4$  g cm $^{-3}$ , and  $T \sim 2 \times 10^8$  K, respectively. For these thermodynamic conditions, a self-sustained detonation propagates in the lateral direction at  $S_D \sim 10^9$  cm s $^{-1}$ , and a laminar deflagration propagates laterally at  $S_L \sim 10$  cm s $^{-1}$  (Timmes 1999).

Purely laminar deflagrations and planar ZND detonations (Zeldovich (see Ostriker 1992); von Neumann 1942; Döring 1943) represent the simplest one-dimensional, steady-state realizations of propagating burning fronts. Hydrodynamic instabilities in deflagrations, some of which are intrinsic to three-dimensional propagating fronts and some of which are related to the buoyancy of the hot burning products with respect to the cold background in the radial direction, give rise to growing perturbations and – unless stabilized by non-linear effects – turbulence. These instabilities deform the combustion surface, potentially altering the structure of the reacting layers. For deflagrations, these instabilities generally increase the rate at which nuclear energy is released. The deformed flame front propagates at a speed faster than a purely laminar flame front as long as the surface area increase dominates over the reduction of local energy generation induced by hydrodynamic strain. For a detonation, these hydrodynamic instabilities generally do not increase either the energy released from burning or the self-sustained detonation speed (e.g., Fickett & Davis 1979). Models for the non-linear evolution of unstable or turbulent combustion fronts often involve statistical tools, and the choice of an appropriate tool requires knowledge of the burning regime of the combustion front.

The main purpose of this paper is to evaluate the regimes of helium burning fronts in the presence of buoyancy-driven (convective) turbulence. A simple dimensional comparison of the relevant length and speed scales of buoyancy-driven turbulence, ZND helium detonations, and laminar helium deflagrations determine whether the combustion front is in the flamelet regime, distributed burning regime, or neither. It will always be assumed in this paper that convective stirring dominates over all other instabilities intrinsic to the flame front. While cellular instabilities behind the detonation front may be relevant in some contexts (Fickett & Davis 1979; Merzhanov & Rumanov 1999), they will not be discussed in this paper.

## 2. Relevant Scales

The physical properties of laminar helium deflagrations, which are primarily determined by a balance between nuclear energy generation and the transport of internal energy, have been evaluated by Timmes (1999) for a large grid of upstream densities and temperatures. We will use the results of this survey for values of the laminar deflagration speeds  $S_L$ , widths  $\delta$ , and density contrasts  $\Delta\rho/\rho$  between the unburned fuel and its ash. The density of the ash is smaller than the density of

the unburned fuel because the density declines behind a subsonic flame front.

There are several plausible definitions for the width of the deflagration. We consider three pragmatic definitions, each of which can be measured by resolved calculations of laminar helium deflagrations. The first definition we consider is the distance between where the temperature is 10% above the upstream temperature and where the nuclear energy generation attains its maximum value. This width is called the reactive width and is denoted  $\delta_{\text{nuclear}}$ . The second width definition we consider is the distance between where the temperature is 10% above the upstream temperature and where the temperature reaches 90% of its downstream value. This width is called the thermal width and is denoted  $\delta_{\text{thermal}}$ . The third definition of a deflagration's width that we consider is the distance between where the composition has its upstream values and where the downstream composition first reaches its final state. This width is called the composition width and is denoted  $\delta_{\text{composition}}$ . For laminar helium deflagrations, the reactive widths  $\delta_{\text{nuclear}}$  are the smallest widths. The thermal widths  $\delta_{\text{thermal}}$  are usually slightly larger than the reactive widths  $\delta_{\text{nuclear}}$ , depending on the upstream thermodynamic conditions. The composition widths  $\delta_{\text{composition}}$  are usually the largest widths, ranging from being 1.2–10 times larger than the thermal widths, depending mainly on the upstream density. We will use the  $\delta = \delta_{\text{nuclear}}$  in our analysis, but qualitatively similar results are obtained if the differences in the widths are taken into account.

The pressure scale height of a hydrostatically stratified helium layer in some cases is comparable to the width of a helium combustion front (e.g., Bildsten 1995), and should be included in any length scale comparisons. The pressure scale height is defined as

$$h_p = \frac{P}{\rho g} \quad (1)$$

where  $P$  is the scalar pressure,  $\rho$  is the mass density, and  $g = GM/R^2$  is the acceleration due to gravity. For the X-ray burst case we assumed a  $M = 1.4M_\odot$  neutron star with a radius of  $R = 10^6$  cm, while for the thin shell instability we the aforementioned model from Iben (1977) that is characterized by  $M \sim 1.0M_\odot$ ,  $R \sim 7 \times 10^8$  cm. The density in both X-ray burst and thin shell instability cases is left as a free parameter, permitting a classification of the helium burning regimes as a function of density.

The amplitude of convective velocity fluctuations on large scales can be estimated by evaluating the terminal rise velocity of buoyant plumes with a diameter  $\sim h_p$  (Layzer 1955):

$$v_b \approx 0.35 \left( g \frac{\Delta\rho}{\rho} h_p \right)^{1/2} = 0.35 \left( \frac{\Delta\rho}{\rho \gamma} \right)^{1/2} v_s, \quad (2)$$

where  $v_s^2 = \gamma P/\rho$  is the local sound speed, and  $\gamma$  is the ratio of specific heats.

For the purpose of classifying turbulent burning regimes, we are interested mainly in the amplitude of turbulent velocity fluctuations at the scale of the combustions front's width (Niemeyer & Kerstein 1997). Assuming that the convectively driven, large scale, fluctuations establish a

turbulent cascade with the exponent  $n$ , we can write

$$v_{\text{turb}}(\delta) = \begin{cases} v_b (\delta/h_p)^n & \text{if } \delta < h_p \\ v_b & \text{otherwise.} \end{cases} \quad (3)$$

The value of  $n$  for buoyancy-driven turbulent cascades is not unambiguously agreed upon. It appears reasonable at present to use either  $n = 1/3$  for Kolmogorov scaling, or  $n = 3/5$  for Bolgiano-Obukhov scaling (Niemeyer & Kerstein 1997). We will assume  $n = 1/3$  Kolmogorov scaling for the remainder of this paper.

### 3. Helium burning regimes

Deflagrations under astrophysical conditions are characterized by the thermal diffusivity  $\kappa$  dominating over all other microscopic transport coefficients, such as viscosity  $\nu$  and mass diffusivity  $D$ . In terms of the dimensionless numbers representing the transport properties of the fluid, the Prandtl number  $Pr = \nu/\kappa$  is very small, and the Lewis number  $Le = \kappa/D$  is very large. As a result of this disparity between the Prandtl and Lewis numbers the conventional classification of turbulent burning regimes (e.g., Bradley 1993), which is based exclusively on time scale criteria, is inappropriate (Niemeyer & Kerstein 1997). It is more appropriate in such astrophysical conditions to combine the length scales and time scales, and compare a turbulent diffusivity  $D_{\text{turb}}(l) \sim v_{\text{turb}}(l) \times l$  with the thermal diffusivity  $\kappa$ . Note the turbulent diffusivity is a function of the length scale being examined. Since  $D_{\text{turb}}$  is a growing function of length scale for most turbulent cascades, it is sufficient for our purposes to consider the largest scale relevant for the flame structure, the flame width  $\delta$ . One may expect that a change of burning regimes occurs when  $D_{\text{turb}} \sim \kappa$  or, equivalently, when  $v_{\text{turb}}(\delta) \sim S_L$ . It must be stressed that these dimensional relationships may have potentially large dimensionless coefficients that can only be determined by experiment or direct numerical simulation.

The regime where  $v_{\text{turb}}(\delta) \ll S_L \ll v_{\text{turb}}(L)$  is generally called the flamelet regime (Peters 1984; Clavin 1994). This regime is characterized by a nearly unperturbed laminar flame structure on small scales and the deformation of the flame surface by turbulent eddies on larger scales. The growth of the flame surface area as a result of turbulent wrinkling increases the energy deposited by nuclear burning, which causes the deformed flame surface to propagate faster than the purely laminar flame front. This turbulent flame speed  $S_T$  should scale linearly with the speed of the fastest (and thus largest) turbulent eddies  $v_{\text{turb}}(L)$  if the conditions for the flamelet region are to hold. In the astrophysical cases of interest here, a reasonable estimate is  $L \approx h_p$ . A number of expressions for the turbulent flame speed  $S_T$  as a function of the turbulent velocity fluctuations have been proposed (e.g., Williams 1985; Yakhot 1988; Pocheau 1994; Shy et al. 1996), but a well-founded consensus has yet to emerge.

The regime where  $v_{\text{turb}}(\delta) \gg S_L$  is known as the distributed burning regime (Peters 1984;

Clavin 1994). This regime is characterized by a deformation of the flame surface even at small scales. Modeling attempts in this regime are severely hampered by the overlapping length and time scales between the turbulent energy transport and nuclear energy generation. Damköhler (1940) proposed a simple re-normalization of the order-of-magnitude estimate for the laminar flame. This re-normalization assumes a vanishing influence of the turbulence on the energy generation rate, which may be unrealistic for distributed burning under astrophysical conditions. Peters (1999) gives an approach to extend flamelet regime models into the distributed burning regime.

The length and speed scales of helium burning are shown in Figures 1 and 2, respectively. Each plot has the upstream (unburned) mass density on the  $x$ -axis, the appropriate scaling variable on the  $y$ -axis. Each curve in the figure is for an upstream composition of pure helium, and an upstream temperature of  $10^8$  K. There are composition effects (the helium mass fraction) and upstream thermodynamic effects (how cold the unburnt fuel is) which determine the exact placement of each curve. However, the magnitude of these two effects are small compared to the scale of the  $y$ -axis and the order of the analysis.

The red curve in Figure 1 shows the purely laminar flame reactive width  $\delta_{\text{nuclear}}$  from the Timmes (1999) survey. Curves for the thermal widths lie almost on top of the red curve, while curves for the composition widths would be displaced toward larger lengths for a given density. The green curve gives the pressure scale height for the X-ray burst case, while the blue curve gives the pressure scale height for the thin shell case. Both pressure scale height curves are from equation (1).

The red curve in Figure 2 shows the laminar flame speed from the Timmes (1999) survey. The green curve gives the buoyancy speed from equation (2). Since the buoyancy speed depends only on local thermodynamic conditions and the local laminar flame properties, the buoyancy speed is identical for both the X-ray burst and the thin shell instability cases. The light blue curve gives the turbulent speed at the scale of the laminar flame’s reactive width for the X-ray burst case, while the dark blue curve gives the same quantity for the thin shell instability. Both turbulent speed curves, evaluated at the scale of the laminar flame reactive width, are calculated from equation (3).

Figure 2 shows the curve for the thin shell turbulent speed crosses the curve for the laminar flame speed at  $\sim 10^7 \text{ g cm}^{-3}$ . At smaller densities the turbulent velocities on the scale of the laminar flame width are larger than the speed of a purely laminar deflagration, which corresponds to the distributed burning regime. In this case, turbulence must be expected to alter the micro-structure of the deflagration flame front as the flame front propagates in either the lateral or radial directions. At densities larger than  $\sim 10^7 \text{ g cm}^{-3}$ , the laminar flame speed is larger than the turbulent speeds on the scale of the laminar flame reactive width, which corresponds to the flamelet regime. In this case, the flame front which propagates in either the radial or lateral directions has a nearly laminar deflagration structure on small scales and a wrinkled surface on larger scales. Turbulent deflagrations travelling in the lateral or radial directions encounter the distributed regime at densities below  $\sim 10^7 \text{ g cm}^{-3}$ , and the flamelet regime at larger densities.

If the thermal deflagration widths are used instead of the reactive widths, the cross-over density is nearly the same since the reactive and thermal widths are of comparable magnitude. If the deflagration composition widths are used instead of the reactive widths, the cross-over density is increased to  $\sim 6 \times 10^7 \text{ g cm}^{-3}$ , since the composition width is generally larger than the reactive width.

Figure 1 shows that the width of purely laminar deflagration becomes larger than the pressure scale height at a density of  $\sim 10^4 \text{ g cm}^{-3}$ . This feature suggests that steady-state laminar deflagrations travelling in the radial direction cannot come into existence at densities smaller than  $\sim 10^4 \text{ g cm}^{-3}$ . At the distributed regime to flamelet regime transition density of  $\sim 10^7 \text{ g cm}^{-3}$ , Figure 1 indicates that the laminar flame reactive width is much smaller than the pressure scale height, suggesting validity of the steady-state assumption for laminar flame propagation in either the lateral or radial directions.

For the X-ray burst case, Figure 2 shows that turbulent speed curve crosses the laminar flame speed curve at  $\sim 10^8 \text{ g cm}^{-3}$ . Below this density a deflagration is in the distributed regime, while at larger densities the deflagration is in the flamelet regime. If the thermal deflagration widths are used instead of the reactive widths, the cross-over density is nearly the same. If the deflagration composition widths are used instead of the reactive widths, the cross-over density is increased to  $\sim 3 \times 10^8 \text{ g cm}^{-3}$ , is not significantly larger than the reactive width at these densities.

Figure 1 shows that the width of purely laminar deflagration becomes larger than the pressure scale height at a density of  $\rho \sim 10^6 \text{ g cm}^{-3}$ . At densities smaller than  $\rho \sim 10^6 \text{ g cm}^{-3}$ , the deflagration structure in the radial direction will look decisively different from steady-state models, even without turbulence. Steady-state laminar deflagrations travelling in the radial direction cannot come into existence at densities smaller than  $\sim 10^4 \text{ g cm}^{-3}$ . While direct simulations are needed to make specific predictions (see Bildsten 1995 for a modest attempt), one may expect that a deflagration propagating in the lateral direction will broaden significantly in the radial direction, and may never even reach a steady state. At the distributed regime to flamelet regime transition density of  $\rho \sim 10^8 \text{ g cm}^{-3}$ , Figure 1 indicates that the laminar flame reactive width is much smaller than the pressure scale height, suggesting validity of the steady-state assumption for laminar flame propagation in either the lateral or radial directions.

For comparison with the turbulent deflagration case, we calculated the structure of planar helium detonations under the ZND theory (Fickett & Davis 1979). Our results for the self-sustained detonation speeds and thermodynamic conditions at the Chapman-Jouguet point agree with the values obtained by Mazurek (1973) and Khokhlov (1988, 1989).

There are several possible definitions for the width of a planar ZND detonation. These include the distance from the shock front to the point where the nuclear energy generation rate attains its maximum value  $W_{\text{nucdot}}$ , the distance from the shock front to the point where the principle fuel has fallen to 1/10 of its initial value  $W_{\text{composition}}$  (Khokhlov 1989), the distance from the shock front to the point where 90% of the total nuclear energy has been released  $W_{\text{nuclear}}$  (Khokhlov 1989),

and the distance from the shock front to where the composition reaches its final nuclear statistical equilibrium state  $W_{\text{NSE}}$ . For planar helium deflagrations, the widths defined by the energy generation rate maximum  $W_{\text{nucdot}}$  are the smallest widths. Depending on the upstream density, the composition widths  $W_{\text{composition}}$ , energy deposition widths  $W_{\text{nuclear}}$ , and nuclear statistical equilibrium widths  $W_{\text{NSE}}$  may be larger than the energy generation rate maximum widths by factors of 1–15. We will use the  $W=W_{\text{nucdot}}$  in our analysis, but qualitatively similar results are obtained if the differences in the various widths are taken into account.

The detonation widths are shown by the purple curve in Figure 1, and the detonation speeds are shown by the purple curve in Figure 2. The speeds of self-sustained detonations, as expected, are much larger than any other speed in Figures 2. Perhaps suprisingly, the width of a self-sustained detonations is larger than the width of a purely laminar deflagration for any given density in Figure 1. For detonations, there is a relatively long time between when material is first heated by the passing shock wave, and when that material begins to burn significantly (the induction time scale of detonations). For deflagrations, there is a relatively short time between when material is first heated by conduction and begins to burn significantly. These time scales, when combined with the fact the speed of a self-sustained detonation is supersonic while the speed of a purely laminar deflagration is very subsonic, explain why the detonation widths are larger than the deflagration widths in Figure 1.

For the X-ray burst case, Figure 1 indicates that the detonation width becomes larger than the the pressure scale height at a density of  $\rho \sim 10^7 \text{ g cm}^{-3}$ . The steady state width is larger than the radial “box” size containing the detonation. This suggests that a steady-state, self-sustained detonations cannot come into existence in the radial direction at densities smaller than  $\rho \sim 10^7 \text{ g cm}^{-3}$ . If the nuclear statistical equilibrium widths are used instead of the reactive widths, the density at which the the width becomes larger than the radial “box” size is increased to  $\sim 6 \times 10^7 \text{ g cm}^{-3}$ .

For the thin shell case, the planar ZND detonation width becomes larger than the pressure scale height at  $\sim 5 \times 10^4 \text{ g cm}^{-3}$ . Steady-state, self-sustained detonations travelling in the radial direction cannot come into existence at densities smaller than  $\sim 5 \times 10^4 \text{ g cm}^{-3}$ .

#### 4. Summary

The various burning regimes encountered by deflagrations and detonations propagating through helium-rich compositions in the presence of buoyancy-driven turbulence have been analyzed, with the main results being shown in Figures 2 and 1.

For turbulent deflagrations in the X-ray burst case, there is a transition from the distributed burning regime to the flamlet regime at a density of  $\sim 10^8 \text{ g cm}^{-3}$ . Turbulent deflagrations propagating in either the lateral or radial directions will be strongly deformed on micro-scales at smaller densities. In addition, the breakdown of the steady-state assumption for laminar deflagrations



propagating in the radial direction is signaled by the laminar deflagration width becoming larger than the pressure scale height at densities smaller than  $\sim 10^6 \text{ g cm}^{-3}$ . This suggests that a purely laminar deflagration cannot come into existence in the radial direction at smaller densities. Similarly, the width of a self-sustained, planar detonation is larger than the pressure scale height at densities less than  $\sim 10^7 \text{ g cm}^{-3}$ , indicating that a steady-state detonation wave cannot come into existence in the radial direction.

Turbulent deflagrations in the thin shell helium flash also encounter both the flamlet and distributed regimes, with the cross-over density being  $\sim 10^7 \text{ g cm}^{-3}$ . Below this cross-over density, flame fronts propagating in the radial and lateral directions are in the flamelet regime, where the flame front has nearly laminar deflagration structure on small scales and a wrinkled surface on larger scales. In addition, the purely laminar deflagration width becoming larger than the pressure scale height at densities smaller than  $\sim 10^4 \text{ g cm}^{-3}$ . Purely laminar deflagration cannot come into existence in the radial direction at smaller densities. Similarly, the width of a planar detonation is larger than the pressure scale height at densities less than  $\sim 5 \times 10^4 \text{ g cm}^{-3}$ . A steady-state self-sustained detonation wave cannot come into existence in the radial direction.

Figures 1 and 2 also have applications towards helping to define what is meant by “resolved” numerical simulations of helium burning.

This work has been supported by the Department of Energy under Grant No. B341495 to the ASCI Center on Astrophysical Thermonuclear Flashes at the University of Chicago.

## REFERENCES

- Bildsten, L. 1995, *ApJ*, 438, 852
- Boisseau, J.R., Wheeler, J.C., Oran, E.S., & Khokhlov, A.M. 1996, *ApJ*, 471, L99
- Bradley D. 1993, 24th Int. Symp. Combust. (Combustion Institute, Pittsburgh), 247
- Brown, E. F. & Bildsten L. 1998, *ApJ*, 496, 915
- Clavin, P., 1994, *Ann. Rev. Fluid. Mech.*, 26, 321
- Clayton, G. C. & De Marco, O. 1997, *AJ*, 114, 2697
- Damköhler, G. 1940, *Z. Elektrochem. angew. phys. Chem.*, 46, 601
- Döring, W., 1943, *Ann. Phys.*, 43, 421
- Fickett, W. & Davis W. C. 1979, *Detonation* (Univ. Calif. Press, Los Angeles)
- Fryxell, B. A., & Woosley, S. E. 1982, *ApJ*, 258, 733

- Fryxell, B. A. & Woosley, S. E. 1982, *ApJ*, 261, 332
- Iben, I. Jr. 1977, *ApJ*, 217, 788
- Khokhlov, A. M. 1988, *ApSS*, 149, 91
- Khokhlov, A. M. 1989, *MNRAS*, 239, 785
- Khokhlov, A. M. 1995, *ApJ*, 449, 695
- Layzer, D. 1955, *ApJ*, 122, 1
- Mazurek, T. J. 1973, *ApSS*, 23, 365
- Merzhanov, A. G. & Rumanov, E. N. 1999, *Rev. Mod. Phys.* 71, 1173
- Montgomery, C. J., Khokhlov, A. M., & Oran, E. S. 1998, *Combust. Flame*, 115, 38
- Niemeyer, J. C. & Kerstein, A. R. 1997, *New Astronomy*, 2, 239
- Ostriker, J. P. 1992, *Selected works of Yakov Borisovich Zeldovich*, (Princeton Univ. Press, Princeton N.J.)
- Paczynski, B. 1974, *ApJ*, 192, 483
- Peters, N. 1984, *Prog. Energy Combust. Sci.*, 10, 319
- Peters, N. 1999, *J. Fluid Mech.*, 384, 107
- Pocheau, A. 1994, *Phys. Rev. E*, 49, 1109
- Schwarzschild, M. & Härm, R. 1965, *ApJ*, 142, 855
- Shy, S. S., Jang, R. H., & Ronney, P. D. 1996, *Combust. Sci. Tech.*, 113, 329
- Taam, R. E. 1987, *Comm. Mod. Phys*, 11, 263
- Taam, R. E., Woosley, S. E., & Lamb, D. Q. 1996, *ApJ*, 459, 271
- Timmes, F. X., & Woosley, S. E. 1992, *ApJ*, 396, 649
- Timmes, F. X. 1999, *ApJS*, in press
- Von Neumann, J., 1942, *OSRD Rep. No.* 549
- Wallace, R. K., Woosley, S. E. & Weaver, T. A. 1982, *ApJ*, 258, 696
- Williams, F. A. 1985, *Combustion Theory* (Benjamin/Cummings, Menlo Park)
- Woosley, S. E. & Taam, R. E. 1976, *Nature*, 263, 101

Yakhot, V. 1988, *Combust. Sci. Tech.*, 60, 191

Zingale et al. 2000, *ApJ*, submitted

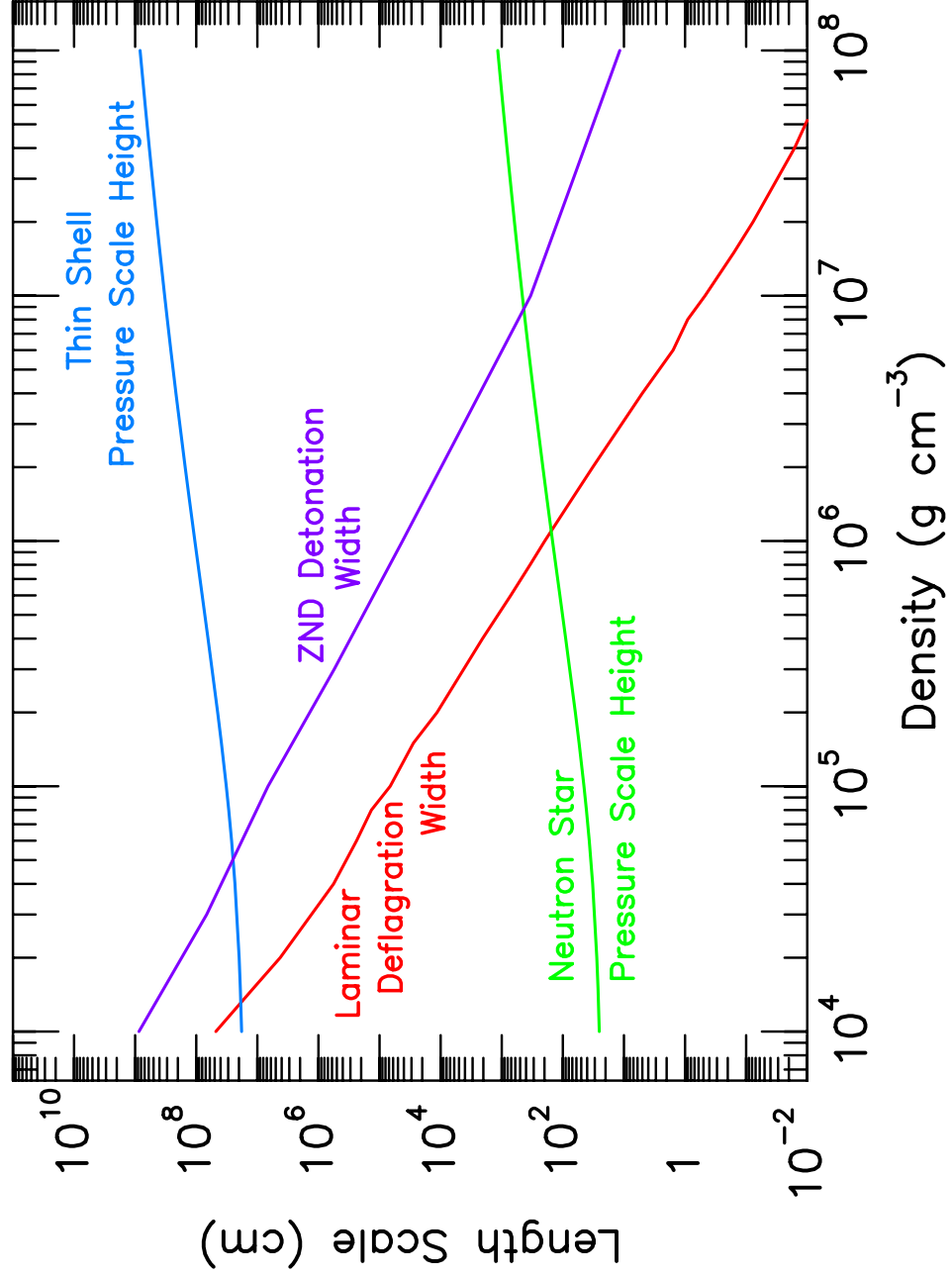


Fig. 1.— Length scales of helium burning. The upstream (unburned) mass density on the  $x$ -axis, and the length scale variable is on the  $y$ -axis.

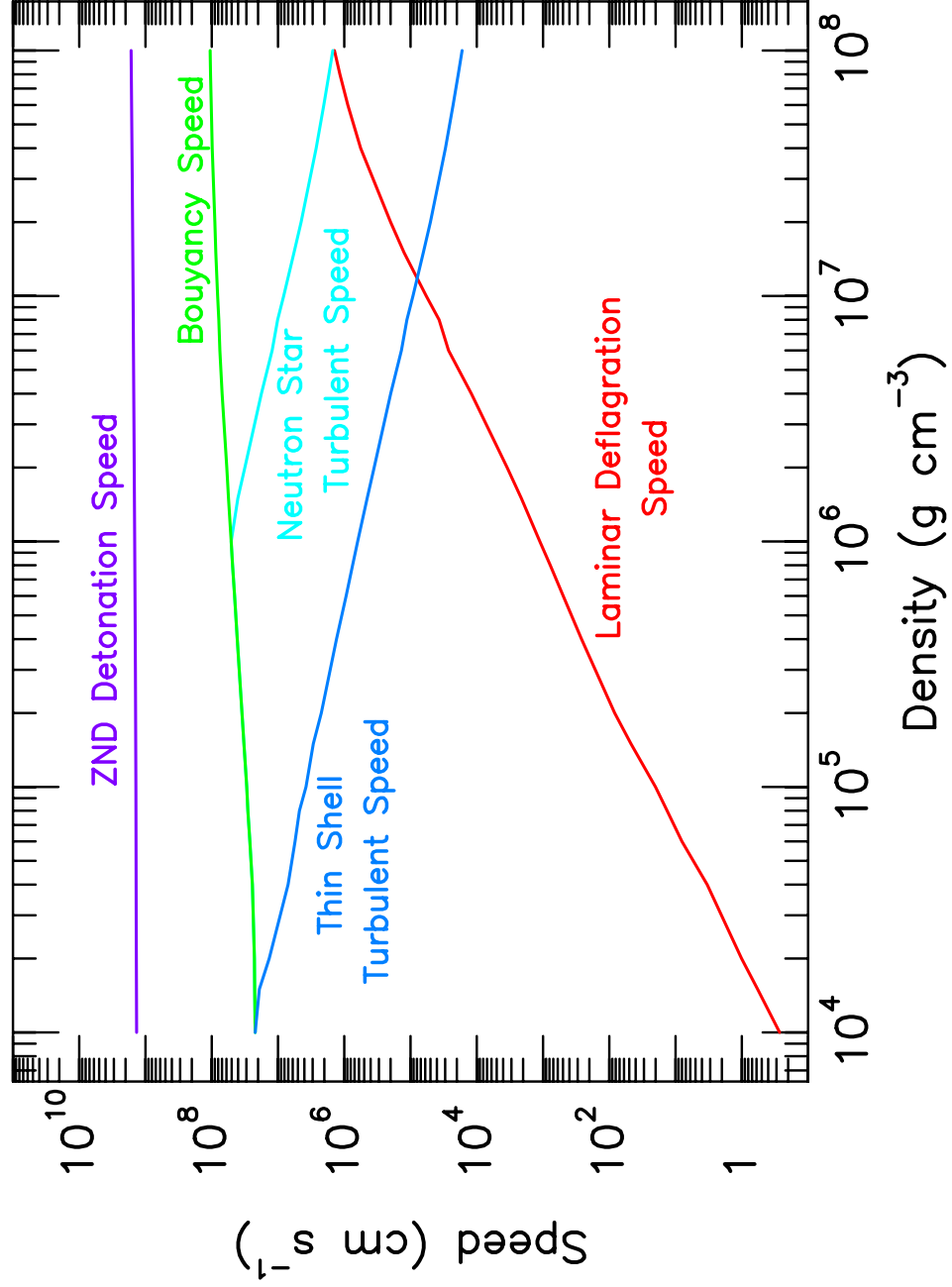


Fig. 2.— Speed scales of helium burning. The upstream (unburned) mass density on the  $x$ -axis, and the speed scaling variable is on the  $y$ -axis.